K_2S-activated carbons developed from coal and their methane adsorption behaviors*

Feng Yan-Yan(冯艳艳), Yang Wen(杨 文), and Chu Wei(储 伟)†

Department of Chemical Engineering, Sichuan University, Chengdu 610065, *China*

(Received 12 February 2014; revised manuscript received 17 April 2014; published online 20 August 2014)

The main purpose of this work is to prepare various activated carbons by K_2S activation of coal with size fractions of 60–80 meshes, and investigate the microporosity development and corresponding methane storage capacities. Raw coal is mixed with K_2S powder, and then heated at 750 °C–900 °C for 30 min–150 min in N_2 atmosphere to produce the adsorbents. The texture and surface morphology are characterized by a N_2 adsorption/desorption isotherm at 77 K and scanning electron microscopy (SEM). The chemical properties of carbons are confirmed by ultimate analysis. The crystal structure and degree of graphitization are tested by X-ray diffraction and Raman spectra. The relationship between sulfur content and the specific surface area of the adsorbents is also determined. K_2S activation is helps to bring about better development of pore texture. These adsorbents are microporous materials with textural parameters increasing in a range of specific surface area 72.27 m^2/g–657.7 m^2/g and micropore volume 0.035 cm^3/g–0.334 cm^3/g. The ability of activated carbons to adsorb methane is measured at 298 K and at pressures up to 5.0 MPa by a volumetric method. The Langmuir model fits the experimental data well. It is concluded that the high specific surface area and micropore volume of activated carbons do determine methane adsorption capacity. The adsorbents obtained at 800 °C for 90 min with K_2S/raw coal mass ratios of 1.0 and 1.2 show the highest methane adsorption capacities amounting to 106.98 mg/g and 106.17 mg/g, respectively.

Keywords: coal, K_2S activation, microporosity, methane adsorption

PACS: 82.80.Dx, 68.43.–h **DOI:** 10.1088/1674-1056/23/10/108201

1. Introduction

Activated carbon (AC) has been recognized as a very promising porous material based on its structure and particular properties, and it is also expected to have many industrial applications[1–4] such as catalysts or catalyst supports,[5] and as energy storage. In addition, AC is the microporous material most widely studied as a potential methane adsorbent.[6–8] The adsorption capacity of methane is governed by the microporous texture of AC. Thus, the porous structure characteristics, including high specific surface area, high pore volume, and appropriate pore size distribution, are the primary requirement for methane adsorption.[9–13] The AC properties depend mainly on the nature of the raw material and the thermal treatment leading to the final ACs.[1,9,14,15] There are many precursors from which ACs can be obtained, such as lignocellulosic materials,[16] coconut shells, olive stones,[9] coal,[2] etc.

ACs with a porous structure tailored for energy storage applications, such as methane storage, could be produced by carefully controlling the activation variables.[10–13] Chemical activation has been shown as an efficient method to obtain carbons with a high specific surface area and appropriate pore size distribution. More recent studies have revealed the effects of the carbonaceous precursor and activation variables on the porous structure of KOH-treated solids, and this procedure is costly due to high KOH/raw material mass ratio when obtaining high specific surface area.[2,3,10–13]

Nowadays, coals, due to their relatively low cost, are among the more important industrial carbons.[17] Compared with ACs, coals show a relatively low surface area.[18] Plenty of investigations on the chemical activation of coals have been performed.[19–22] A particular coal with a higher surface area is expected to show better performance in wider applications.[23,24] Wajima and Sugawara[2] investigated the coal activated by K_2S to develop the porosity for mercury adsorption from aqueous solution, but the results showed that the maximum surface area was below 50 m^2/g. The mechanism of porosity generation with K_2S activation involves the oxidation of coals, followed by potassium metal intercalation between the graphene layers of carbonaceous materials.[10–13] Potassium penetration, depending on the precursor nature, is responsible for carbon particles breaking.[2,3,10–13] The results have shown that strong cross-links between basic structural units (BSU) of the coal allow particle integrity to be partially preserved.[2,25]

The above description has become our motivation to study K_2S activation of coal as a potential route to high surface area activated carbons with low K_2S/raw coal mass ratios. Therefore, in this study we focus on the structural changes of coal according to the development of pore texture through K_2S activation. The first part is to select the suitable heating temperature of raw coal, based on the texture of the produced activated carbons. The second part is to focus on op-

*Project supported by the National Basic Research Program of China (Grant No. 2011CB201202).

†Corresponding author. E-mail: chuwei1965scu@163.com

© 2014 Chinese Physical Society and IOP Publishing Ltd

timizing the heating time in terms of microporosity development of activated carbons, based on the selected heating temperature. The third part is to deal with the effect of various K_2S/raw coal mass ratios on the texture of the resultant carbons. The morphologies and structures of activated coals are observed under N_2 adsorption/desorption and scanning electron microscopy (SEM). Crystallographic parameters of activated carbons are also examined with X-ray diffraction (XRD) and Raman spectroscopy in order to understand the structural changes. A methane adsorption test is performed to examine the adsorption properties of the produced K_2S-activated carbons compared with raw coal under pressures up to 5.0 MPa.

2. Experiment

2.1. Preparation

The coal sample used in this study was available from Chenjiashan Coalmine, Shanxi, China. Raw coal was dried, crushed, and sieved to particle sizes of 60–80 meshes. Table 1 shows the proximate and ultimate analyses of raw coal.

Table 1. Chemical analyses of raw coal (air-dried basis, mass fraction, %).

	Proximate analysis			Ultimate analysis				
Properties	Ash	Fixed carbon	Volatile matter	C	H	N	S	O*
Value	9.08	59.38	31.54	72.76	4.95	< 0.5	4.48	> 17.31

O*: by difference.

(i) **Pyrolysis with K_2S at various temperatures**

A 3.0-g raw coal was mixed with 2.7 g of K_2S powder (0.9 of the K_2S/raw coal mass ratio), and the mixture was placed in a horizontal reactor, the temperature of which was controlled by an electric furnace. The reactor with an N_2 atmosphere was heated, separately, at 750, 800, 850, and 900 °C for 30 min to pyrolyze the sample. After pyrolysis, the product was cooled to room temperature in an atmosphere of N_2. Particles were washed repeatedly with distilled water, and dried at 110 °C for 12 h. The adsorbents prepared separately at 750, 800, 850, and 900 °C were abbreviated as S-750-30-09, S-800-30-09, S-850-30-09, and S-900-30-09, respectively.

(ii) **Pyrolysis with K_2S at various times**

The best sample with a high specific surface area was chosen to investigate the effect of heating time. Based on the preceding treatment, a temperature of 800 °C was chosen as the heating temperature, and the heating times were 30, 90, and 150 min, respectively. Others were similar to the above. The adsorbents prepared for 30, 90, and 150 min at 800 °C were named as S-800-30-09, S-800-90-09, and S-800-150-09, respectively.

(iii) **Pyrolysis with K_2S at various K_2S/raw coal mass ratios**

The sample was heated at 800 °C for 90 min, and the K_2S/raw coal mass ratio was varied from 0.0 to 1.2. The resulting materials were labeled as S-800-90-00, S-800-90-03, S-800-90-06, S-800-90-09, S-800-90-10, and S-800-90-12, respectively.

2.2. Characterization

The ultimate analysis of samples was performed in a CARLO ERBA 1106 element analyzer (Italy). The oxygen content was calculated by difference.[26]

The textural characterization of the samples was performed by N_2 adsorption/desorption isotherms, determined at 77 K with a NOVA1000e surface area and pore size analyzer (Quantachrome Company).[18,26] Specific surface areas and pore size distributions of the samples were measured by the Brunauer–Emmett–Teller (BET) method and HK method, respectively. The micropore volume was determined by HK method and the total pore volume was evaluated at $p/p_0 = 0.98 \sim 0.99$.

Surface morphology was investigated by scanning electron microscopy (SEM) (Hitachi S-4800, Japan).

The X-ray diffractograms of the samples were recorded in a DX-1000 powder diffractometer equipped with a Cu Kα X-ray source and an internal standard of silicon power.[18]

The Raman spectra of the samples were measured with a Raman microspectrometer (Renishaw System InVia) using an argon laser as the excitation source ($\lambda = 514.5$ nm). The spectra were recorded in a wave number range of 4×10^2 cm^{-1} $\sim$ 4×10^3 cm^{-1}.[18,21]

2.3. Methane adsorption

Methane adsorption measurements were conducted using a volumetric method similar to that described previously.[18,21,24–26] Since helium cannot be adsorbed at pressures below 10 MPa, it was usually used for the void volume calibration in the adsorption setup. Prior to helium calibration, approximately 5.0 g[25–27] of the sample dried overnight at 383 K, was evacuated in the adsorption cell and the cell sections were kept at the required temperature using an isothermal oven. The detailed experimental steps were similar to those described in the literature.[18,21,25] The purities of helium and methane were 99.999% and 99.99% respectively. A methane adsorption test was operated under pressure ranges of 0–5.0 MPa at 298 K. The adsorption process was repeated twice to guarantee the validity of the experiment.

3. Results and discussion

3.1. Textural and structural characteristics

The effects of heating temperature, heating time, and K_2S/raw coal mass ratio on the textural characteristics of coals in K_2S activation are shown in Fig. 1, Table 2, and Fig. 2, respectively.

Figure 1 shows the N_2 adsorption/desorption isotherms of the samples. All of the isotherms have similar shapes, and exhibit remarkable hysteresis loops, indicating that the mesoporous structures are maintained. The adsorption and desorption curves do not coincide at a low relative pressure, revealing that pyrolysis with K_2S has different effects on the improvement in pore structures. As shown in Fig. 1(a), the volume amount adsorbed (cm^3/g) increases to a maximum and then decreases with increasing heating temperature, a trend which is similar to those of the adsorbents prepared at various heating times (shown in Fig. 1(b)). Figure 1(c) displays the N_2 adsorption/desorption isotherms of the samples with different K_2S/raw coal ratios, indicating that through the pyrolysis with K_2S, we can develop the pore structure of the adsorbent by increasing the K_2S/raw coal ratio.

The pore parameters of activated carbons prepared under different experimental conditions are presented in Table 2. The results indicate that the S_{BET} depends on the pyrolysis parameters, namely the heating temperature, the heating time, and the mass ratio of K_2S and the raw coal. The value of the specific surface area of S-800-90-00 without K_2S activation is very small, 0.446 m^2/g, while the raw coal is 5.808 m^2/g of the specific surface area. The highest specific surface area of K_2S pyrolysis carbons is 657.7 m^2/g, which is 113 times as high as that of raw coal. In addition, the BET specific surface areas of obtained activated carbons are much higher than the results of Wajima and Sugawara,[2] which are all below 50 m^2/g. For various heating temperatures, the S_{BET} initially increases to a maximum value of 487.1 m^2/g at 800 °C, and then decreases with the increase of heating temperature. The increase is due to an increase in the volatile release of the raw coal, which helps to develop the pore structure and increase the pore surface area. However, further increasing the heating temperature leads to a pronounced decrease of S_{BET} and micropore volume, which is also proved by N_2 adsorption/desorption isotherms (Fig. 1(a)).

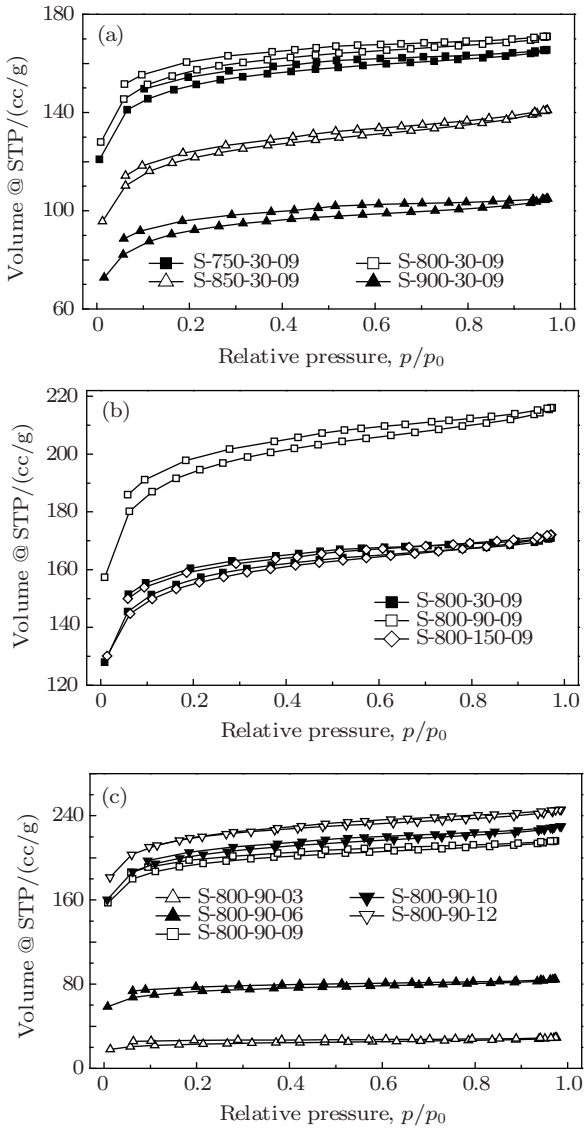


Fig. 1. N_2 adsorption/desorption isotherms (77 K) of the samples prepared under different conditions.

Table 2. Textural characteristics obtained by N_2 adsorption analyses of the samples.

Sample	Specific surface area, BET/(m^2/g)	Micropore volume, HK/(cm^3/g)	Total pore volume/(cm^3/g)	Average pore diameter/nm
S-750-30-09	469.7	0.229	0.256	2.179
S-800-30-09	487.1	0.238	0.264	2.172
S-850-30-09	379.9	0.184	0.218	2.296
S-900-30-09	287.9	0.139	0.162	2.253
S-800-90-09	603.2	0.295	0.334	2.215
S-800-150-09	480.9	0.236	0.266	2.214
S-800-90-00	0.446	–	0.0034	–
S-800-90-03	72.27	0.035	0.045	2.486
S-800-90-06	228.0	0.111	0.131	2.291
S-800-90-10	610.2	0.307	0.356	2.333
S-800-90-12	657.7	0.334	0.380	2.313
Raw coal	5.808	0.0023	0.0093	6.434

The effects of heating times ranging from 30 min to 150 min are studied, and the results are displayed in Table 2. The S_{BET} and micropore volume of the adsorbents start to increase with a heating time lower than 90 min (the heating temperature is 800 °C). When activated at 90 min, the S_{BET} and micropore volume of the sample change remarkably: S_{BET} reaches a maximum value at 603.2 m^2/g surface area, which is more than 100 times higher than that of the raw coal. The sharp decrease in the BET surface area and micropore volume at higher heating time (150 min) may be due to the contraction or collapse of pores, which leads to the reduction in porosity development.

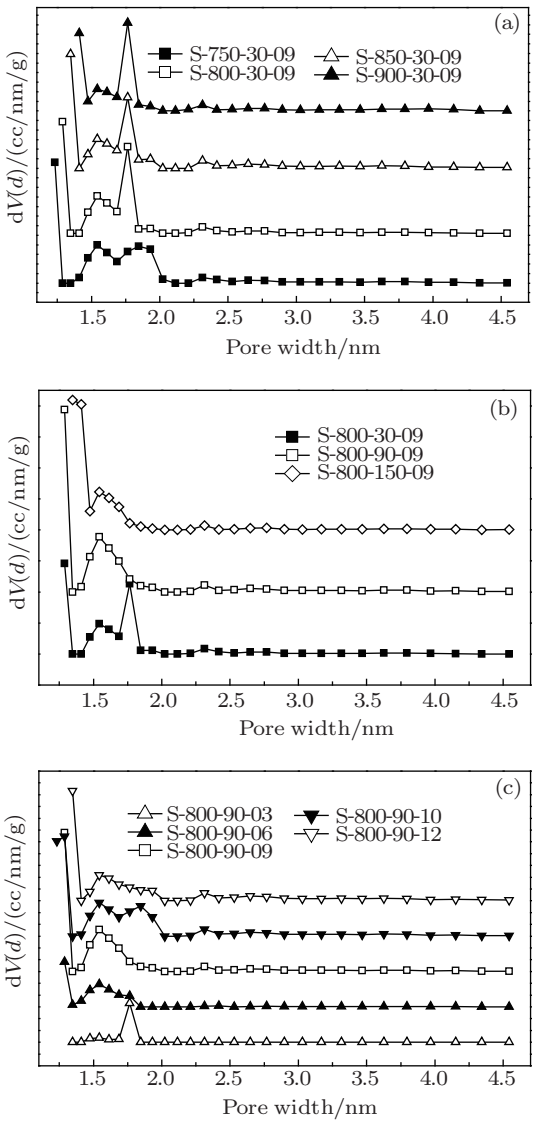


Fig. 2. Pore size distributions obtained from the HK equation.

The BET specific surface area clearly varies in the range of 0.446 m^2/g–603.2 m^2/g as the mass ratio of K_2S to raw coal (heating temperature is 800 °C, and heating time is 90 min) increases from 0.0 to 0.9. When the K_2S/raw coal ratio increases higher than 0.9, the S_{BET} of the adsorbents slightly increases. It can be concluded that the first effect of K_2S is to destruct the carbon matrix of the raw coal, and the high specific surface area is due to the intercalation of potassium compounds. Both the micropore volume and the total pore volume show the same trends as the development trends of the specific surface area of the samples.

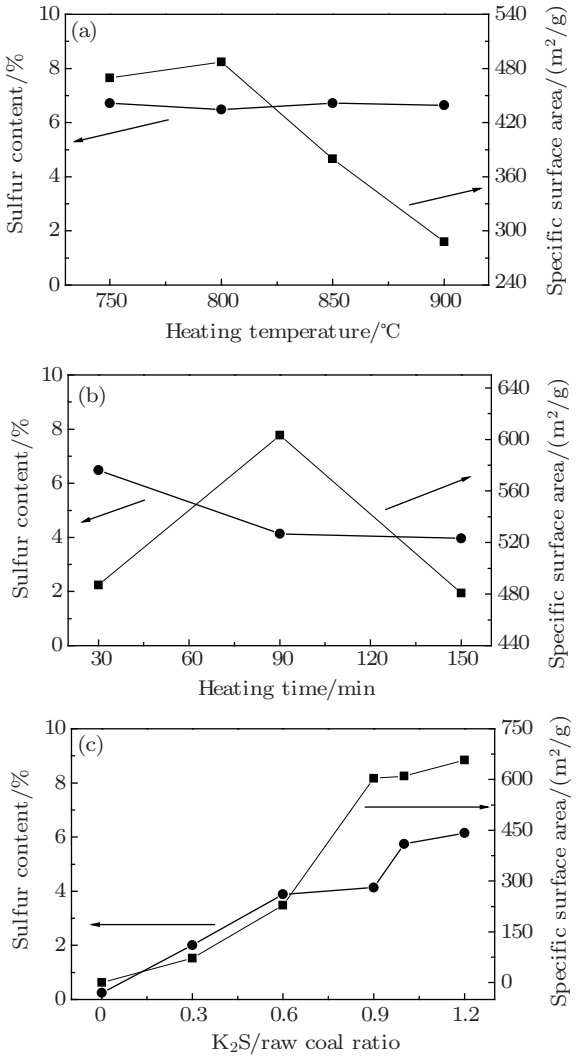


Fig. 3. Sulfur content values and specific surface areas of the adsorbent prepared by pyrolysis with K_2S at various temperatures (a), various times (b), and various K_2S/raw coal mass ratios (c).

Evolution of the adsorbent porosity is studied by the HK method. The pore size distributions demonstrated in Fig. 2 show that the pore structures of the specimens are predominantly microporous structures with a number of mesopores. For various heating temperatures, the pore volumes of the heated specimens shift to the left side. When treated at 800 °C, the sample S-800-30-09 exhibits more micropores within the microporous range (< 2 nm) than the other three samples. One can expect that due to a higher temperature of the preceding treatment, the AC is more sensitive to K_2S activation. For various heating times, the adsorbents shift to smaller micropores, and the sample S-800-90-09 possesses the most micropores in the samples prepared at different heating times (the heating temperature is 800 °C). When the sample is heated at 800 °C

for 90 min, the pore size distributions, shown in Fig. 2(c), depend on the K_2S/raw coal mass ratio, that is, the increase in the K_2S/raw coal mass ratio results in different developments of micropores. Indeed, the enhancement in porosity can be explained by the formation of K-compounds in the carbon matrix, which leads to the destruction of carbon lamellae.

Figure 3 displays the sulfur content values and specific surface areas of the adsorbent prepared by pyrolysis. As shown in Fig. 3(a), sulfur content values of all adsorbents obtained at 750, 800, 850, and 900 °C increase to approximately 6.7 wt%, and are almost the same regardless of pyrolysis temperature, indicating that pyrolysis with K_2S at 750 °C–900 °C can be achieved to impregnate the possible amount of sulfur into coal under the experimental conditions. Specific surface area of the adsorbents is higher than that of raw coal (5.808 m^2/g), due to the pyrolysis with K_2S. The specific surface area increases to 487.1 m^2/g, with the heating temperature of pyrolysis increasing to 800 °C, and then decreasing from 487.1 m^2/g to 287.9 m^2/g as the heating temperature further increases. Sulfur content values of the obtained adsorbents at various heating times 30, 90, 150 min decrease (Fig. 3(b)), while the specific surface area increases to a maximum value of 603.2 m^2/g at 90 min. As shown in Fig. 3(c), with the K_2S/raw coal ratio increasing from 0.0 to 1.2, the specific surface area increases in the range of 0.446 m^2/g–657.7 m^2/g, as does the sulfur content.

Figure 4 shows the SEM images of the five typical samples. The surface of raw coal is smooth with few fragments. In the case of K_2S pyrolysis, the raw coal charred and carbonized the carbon skeleton with the creation of a porous structure. The surface of S-800-90-00 became wrinkled, and S-800-30-09, S-800-90-09, and S-800-90-12 with honeycomb voids contained an irregular, heterogeneous, and highly porous surface, illustrating the development of micropores. Depending on the heating time, the external surfaces of S-800-30-09 and S-800-90-09 have pores with different sizes and shapes as shown in Figs. 4(a) and 4(b), respectively. However, as the mass ratio of K_2S to raw coal increases from 0.9 to 1.2, the number of pores increases, and the pores become smaller as shown in Figs. 4(b) and 4(d), respectively, which is consistent with the results of N_2 adsorption/desorption measurements.

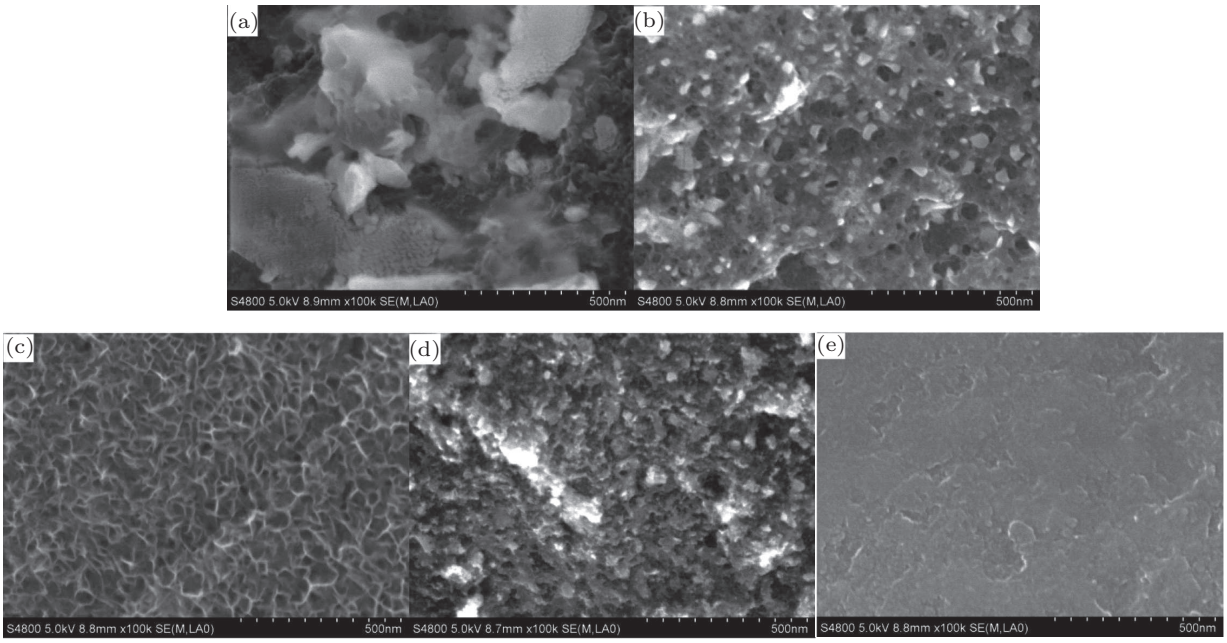


Fig. 4. SEM images of S-800-30-09 (a), S-800-90-09 (b), S-800-90-00 (c), S-800-90-12 (d), and raw coal (e).

Carbon materials are analyzed by X-ray diffraction to study their structures and degrees of order. Figure 5 shows the XRD patterns of the samples prepared from the coal. A carbon 002 reflection is included in the range of 2θ. With raising the heating temperature up to 900 °C, there appear two broad peaks at around 25° and 45° of the adsorbents, attributed to the (002), and (100) characteristics planes of graphite. Depending on the pyrolysis treatment, the main XRD peak, (002), appears to be a superposition of a broader peak and a narrow one, suggesting that the samples contain a certain amount of amorphous carbon. For various heating times, the two broad peak intensities increase significantly as the activation time increases from 30 min to 150 min, which indicates an increase in crystallite size or content of the ordered carbon formed. For various K_2S/raw coal mass ratios, the broad 002 peak is found to be located around $2\theta = 25°$ for each of all the samples,

which is shown in Fig. 5(c), and the 002 peak is sharper and stronger for either of the samples S-800-90-00 without K_2S activation and raw coal. For any of other samples, both the position and the shape of the peak are changed little.

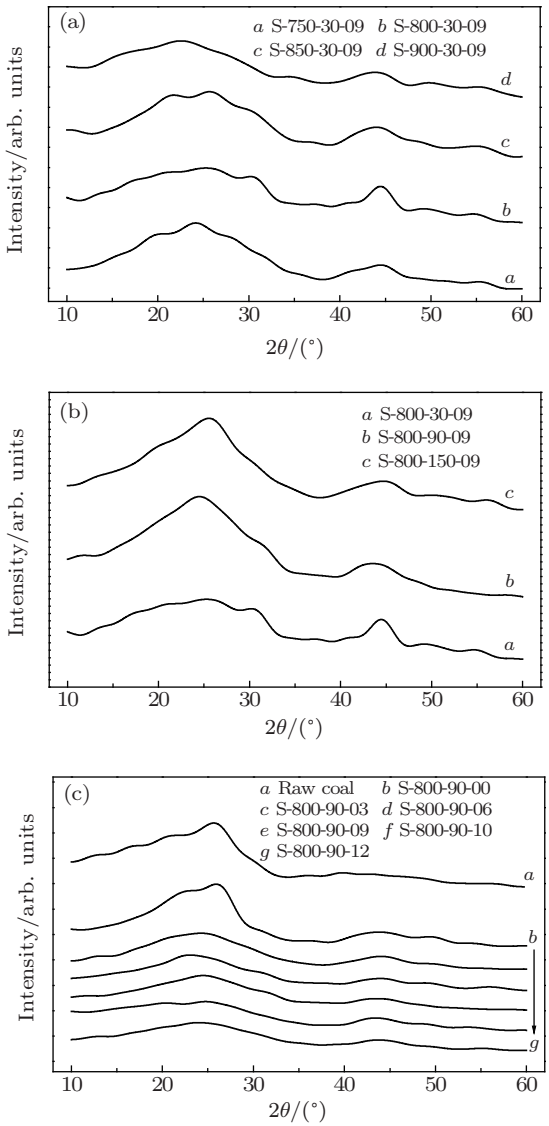


Fig. 5. XRD patterns of the samples studied.

The Raman spectra of the five typical samples, shown in Fig. 6, are characteristic of highly oriented carbon materials with the first-order (1200 $cm^{-1} \sim 1700$ cm^{-1}, a prominent G band at 1590 cm^{-1}, and a less-intense D band at 1350 cm^{-1}) and second-order (2500 $cm^{-1} \sim 2900$ cm^{-1}).[18,28] The second-order Raman spectrum shows the G′ band which is characteristic of tridimensionally ordered material.[18,28] The peak at 1590 cm^{-1} (G band) corresponds to the E_{2g} mode of hexagonal graphite and is related to the vibration of the sp^2-hybridized carbon atoms in a graphite layer. This implies that the adsorbents are composed of graphitic carbon atoms, which is consistent with the XRD results. The D band at approximately 1350 cm^{-1} is associated with the vibration of carbon atoms with dangling bonds in the plane terminated by disordered graphite. The value of I_D/I_G of the sample S-800-90-00 increases compared with that of raw coal, indicating the relative increase in the concentration of aromatic rings results from the release of hydrocarbons after the heat treatment. For the samples pyrolyzed with different heating times but the same heating temperature and K_2S/raw coal mass ratio, as the heating time increases, I_D/I_G varies from 0.897 to 0.847, showing no obvious change. However, various K_2S/raw coal mass ratios each exert a significant influence on the value of I_D/I_G. With the K_2S/raw coal mass ratio increasing from 0.0 to 1.2, I_D/I_G rises from 0.793 to 0.893.

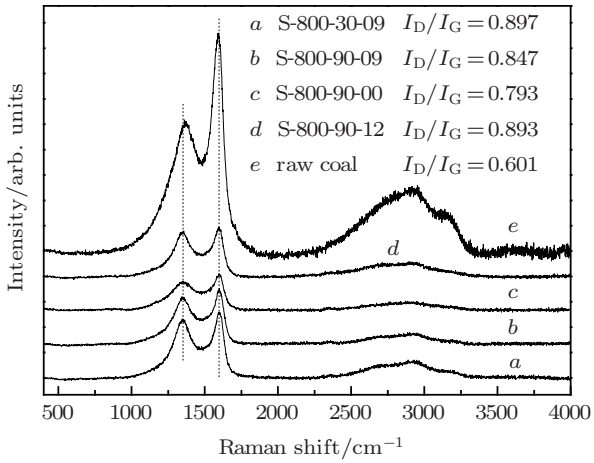


Fig. 6. Raman spectra for the typical samples.

During the pyrolysis, K_2S first decomposes, and then forms the complex salts at the carbon surface, which act as 'active sites'. These compounds cause the separation of carbon lamellae by the oxidation of cross-linking carbon atoms and the formation of surface groups on the edge of the lamellae, which are considered to cause the loss of the flat form and the presence of amorphous or low-organized carbon between the crystallites. As the washing removes these compounds, the structure cannot return to the original form. Due to the presence of amorphous or low-organized carbon over the adsorbent surface, the structure of the sample becomes disordered, thus leading to an increase of I_D/I_G, which is consistent with the results of N_2 adsorption/desorption measurements, SEM images, and XRD.

3.2. Methane adsorption

ACs produced from coals at different heating temperatures, heating times, and K_2S/raw coal mass ratios are assessed as adsorbents under pressures up to 5.0 MPa at 298 K by the volumetric method. The experimental data are graphically presented in Fig. 7. The adsorption isotherms obtained on the samples are found to belong to the characteristic type I morphology according to the IUPAC classification.[18,24–26,29] The capacity of methane adsorption continues to increase rapidly

up to 0.7 MPa∼2.0 MPa, but then increases slowly with the pressure further rising as reported previously.

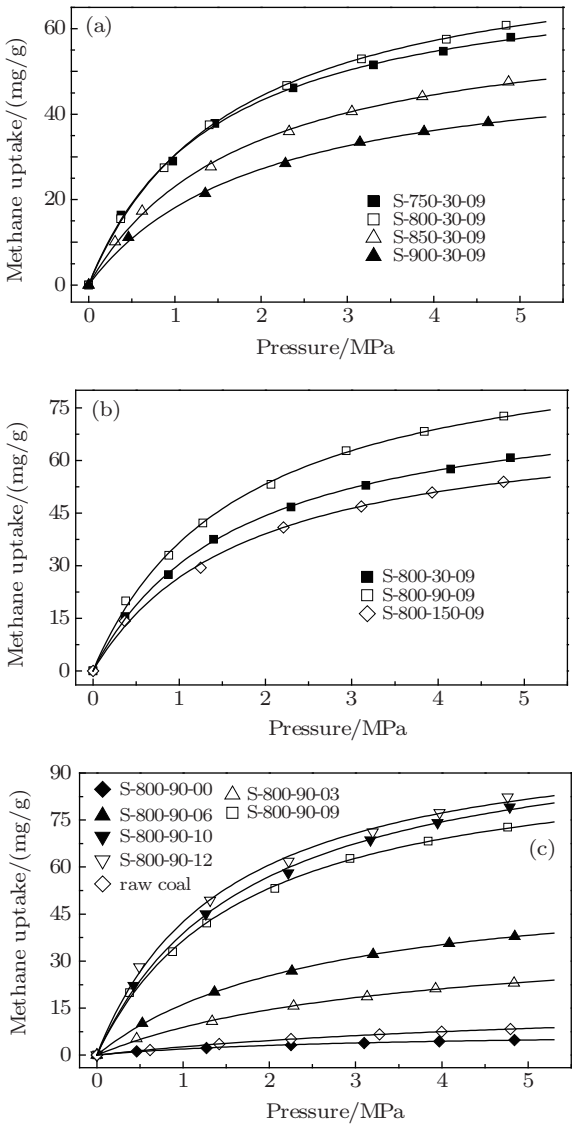


Fig. 7. Methane adsorption isotherms at 298 K, obtained by using the volumetric method, and the solid lines represent the results from the Langmuir model.

The methane adsorption isotherms in Fig. 7(a) show that the S-800-30-09 and S-900-30-09 activated carbons have the highest and lowest methane uptakes in the four samples, respectively. With increasing the heating temperature, the methane uptake reached a maximum, from 74.56 mg/g to 80.93 mg/g (Table 3), however when the activated temperature is higher than 800 °C, the adsorption capacity decreases to 54.19 mg/g. It is concluded that the loss of methane uptake is associated with carbonization above 800 °C. Figure 7(b) shows the adsorption isotherms of methane onto the activated carbons prepared with various heating times. The order of the storage quantity of activated carbons is almost the same as the order of the BET specific surface area and micropore volume listed in Table 2, so is the trend of the adsorption data onto the activated carbons prepared with various K_2S/raw coal mass ratios as shown in Fig. 7(c).

Table 3. Langmuir parameters of equilibrium isotherms obtained from the Langmuir model.

Sample	*a*/(mg/g)	*b*/MPa^{-1}
S-750-30-09	74.56	0.687
S-800-30-09	80.93	0.603
S-850-30-09	64.54	0.556
S-900-30-09	54.19	0.502
S-800-90-09	97.95	0.595
S-800-150-09	73.62	0.566
S-800-90-00	7.65	0.343
S-800-90-03	39.32	0.292
S-800-90-06	57.78	0.390
S-800-90-10	106.98	0.570
S-800-90-12	106.17	0.667
Raw coal	18.98	0.163

Previous studies have shown that BET specific surface area and micropore volume are main factors in gas adsorption.[22,24,30] As displayed in Fig. 8, the samples with higher BET specific surface area and micropore volume possess a higher methane adsorption capacity, which is consistent with the results of previous studies.[24]

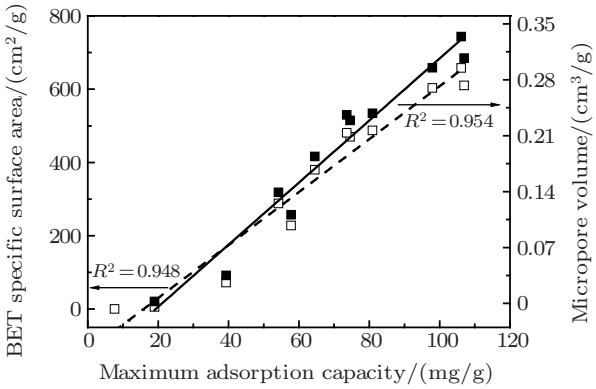


Fig. 8. Variations of BET specific surface area and micropore volume with maximum adsorption capacity.

In addition, although the BET specific surface areas and micropore volumes of the samples S-750-30-09, S-800-30-09, and S-800-150-09 are similar, the methane adsorption capacities are different. Combining with the pore size distributions, the sample S-800-30-09 with a narrower, sharper, and greater micropore size distribution displays a better methane storage ability. The pore size distributions of S-750-30-09 and S-800-150-09 are broader and more dispersed. For S-800-150-09, the aggressive activation leads to the decrease in the number of micropores. It is concluded that the methane storage on the activated carbons increases as the BET specific surface area and the micropore volume increase.[30] When the BET specific surface area and the micropore volume of the specimen are considerable, the micropore size distribution is a more decisive factor. The more favorable the micropore size distribution, the better the amount of methane uptake is. These indicate that the difference in pore structure should explain the methane adsorption behavior.

Furthermore, the experimental data of methane adsorbed on the activated carbons obtained by the volumetric method are compared with literature data,[24,30–32] and the methane uptake of the available activated carbons at 298 K from the cited literature is shown in Fig. 9. The data of the energy density of methane storage according to our results are much higher than the data from the cited literature, indicating the produced activated carbons are very suitable for methane storage vis-a-vis the activated carbons prepared by the cited literatures.

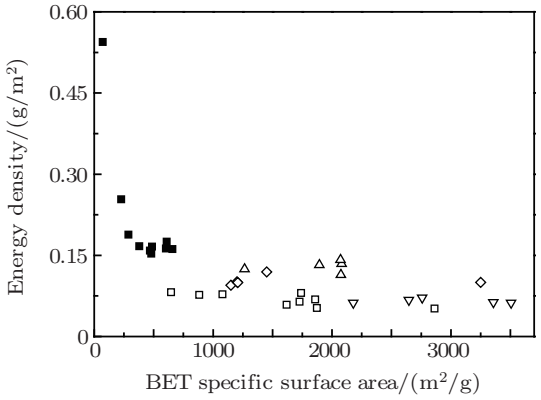


Fig. 9. Experimental curve of energy density (g/m^2) versus BET specific surface area compared with the literature data. ■: in this work.

4. Conclusions

Microporous activated carbons with acceptable microporosity are successfully prepared using K_2S activation of coals with particle sizes of 60–80 meshes. The pyrolysis temperature does not seem to have as important an effect on the porous texture under the conditions studied. While elevating the activated temperature of the coal achieves a maximum in the porosity development at 800 °C, the resulting activated carbons at each of various heating times present a maximum in pore development when heated for 90 min as well. ACs prepared by heat treatment at 800 °C for 90 min are microporous materials with porous texture parameters increasing as the K_2S/raw coal ratio increases from 0.0 to 1.2. Since the K_2S/raw coal ratio increases, the microporosity widens, leading to an increased micropore volume and a more heterogeneous micropore size distribution. As the suitable activated carbons used for methane storage are prepared from a cheap and abundant precursor (coal) by only one activation step, experimental methane adsorption capacity as high as 106.98 mg/g can be obtained for the sample S-800-90-10.

In addition, in this work the importance of pore texture for the methane adsorption capacity is indicated. It is seen that a sample with a higher BET specific surface area and micropore volume presents a higher methane uptake. While the BET specific surface areas and micropore volumes of the samples are considerable, a sample with a large proportion of pores with the optimum size exhibits a higher methane adsorption capacity. Thus, with these results it is demonstrated that the methane adsorption capacity is dependent not only on the BET specific surface area and micropore volume but also strongly on the micropore size distribution.

References

[1] Wu F C, Tseng R L and Juang R S 2005 *Sep. Purif. Technol.* **47** 10
[2] Wajima T and Sugawara K 2011 *Fuel Process. Technol.* **92** 1322
[3] Kierzek K, Frackowiak E, Lota G, Gryglewicz G and Machnikowski J 2004 *Electrochim. Acta* **49** 515
[4] Rangel-Mendez J R and Cannon F S 2005 *Carbon* **43** 467
[5] Yang W, Chu W, Jiang C F, Wen J and Sun W J 2011 *Chin. J. Catal.* **32** 1323
[6] Feng Y Y, Chu W and Sun W J 2012 *Journal of China Coal Society* **37** 1488
[7] Liu F S, Chu W, Sun W J, Xue Y and Jiang Q 2012 *J. Nat. Gas Chem.* **21** 708
[8] He M C and Zhao J 2013 *Chin. Phys. B* **22** 016802
[9] Ubago-Pérez R, Carrasco-Marín F, Fairén-Jiménez D and Moreno-Castilla C 2006 *Micropor. Mesopor. Mat.* **92** 64.
[10] Raymundo-Piñero E, Azaïs P, Cacciaguerra T, Cazorla-Amorós D, Linares-Solano A and Béguin F 2005 *Carbon* **43** 786
[11] Wajima T, Murakami K, Kato T and Sugawara K 2009 *J. Environ. Sci.* **21** 1730
[12] Król M, Gryglewicz G and Machnikowski J 2011 *Fuel Process. Technol.* **92** 158
[13] Raymundo-Piñero E, Kierzek K, Machnikowski J and Béguin F 2006 *Carbon* **44** 2498
[14] Ji Y, Li T, Zhu L, Wang X and Lin Q 2007 *Appl. Surf. Sci.* **254** 506
[15] Górka J, Zawislak A, Choma J and Jaroniec M 2008 *Carbon* **46** 1159
[16] Díaz-Terán J, Nevskaia D M, Fierro J L G, López-Peinado A J and Jerez A 2003 *Micropor. Mesopor. Mat.* **60** 173
[17] Bae J S, Bhatia S K, Rudolph V and Massarotto P 2009 *Energ. Fuel* **23** 3319
[18] Feng Y Y, Jiang C F, Liu D J and Chu W 2013 *J. Anal. Appl. Pyrol.* **104** 559
[19] Chen Y, Wang X and He R 2011 *Fuel* **90** 499
[20] González D, Montes-Morán M A and Garcia A B 2003 *Energ. Fuel* **17** 1324
[21] Feng Y Y, Jiang C F, Liu D J and Chu W 2014 *Chin. Phys. B* **23** 028201
[22] Perrin A, Celzard A, Albiniak A, Kaczmarczyk J, Marêcché J F and Furdin G 2004 *Carbon* **42** 2855
[23] Takagi H, Maruyama K, Yoshizawa N, Yamada Y and Sato Y 2004 *Fuel* **83** 2427
[24] Luo J J, Liu Y F, Jiang C F, Chu W, Jie W and Xie H P 2011 *J. Chem. Eng. Data* **56** 4919
[25] Feng Y Y, Yang W, Liu D J and Chu W 2013 *Chin. J. Chem.* **31** 1102
[26] Hao S X, Wen J, Yu X P and Chu W 2013 *Appl. Surf. Sci.* **264** 433
[27] Busch A, Gensterblum Y, Krooss B M and Siemons N 2006 *Int. J. Coal Geol.* **66** 53
[28] Celorrio V, Calvillo L, Pérez-Rodríguez S, Lázaro M J and Moliner R 2011 *Micropor. Mesopor. Mat.* **142** 55
[29] Wang X L, French J, Kandadai S and Chua H T 2010 *J. Chem. Eng. Data* **55** 2700
[30] Lozano-Castello D, Alcaniz-Monge J, Casa-Lillo M A, Cazorla-Amoros D and Linares-Solano A 2002 *Fuel* **81** 1777
[31] Lozano-Castello D, Cazorla-Amoros D, Linares-Solano A and Quinn D 2002 *Carbon* **40** 989
[32] Himeno S, Komatsu T and Fujita S 2005 *J. Chem. Eng. Data* **50** 369